



Contents lists available at ScienceDirect

Nuclear Instruments and Methods in Physics Research A

journal homepage: www.elsevier.com/locate/nima

Results from a beam test of silicon strip sensors manufactured by Infineon Technologies AG



M. Dragicevic^{a,*}, G. Auzinger^{a,b}, U. Bartl^c, T. Bergauer^a, S. Gamberith^c, J. Hacker^c,
A. König^{a,c}, F. Kröner^c, E. Kucher^c, J. Moser^c, T. Neidhart^c, H.-J. Schulze^d,
W. Schustereder^c, W. Treberspurg^a, T. Wübben^c

^a Institute of High Energy Physics, Austrian Academy of Sciences, Vienna, Austria

^b CERN, Geneva, Switzerland

^c Infineon Technologies Austria AG, Villach, Austria

^d Infineon Technologies AG, Munich, Germany

ARTICLE INFO

Available online 26 April 2014

Keywords:

Silicon sensor

Planar strip sensor

P-on-n

Semiconductor production

ABSTRACT

Most modern particle physics experiments use silicon based sensors for their tracking systems. These sensors are able to detect particles generated in high energy collisions with high spatial resolution and therefore allow the precise reconstruction of particle tracks. So far only a few vendors were capable of producing silicon strip sensors with the quality needed in particle physics experiments. Together with the European-based semiconductor manufacturer Infineon Technologies AG (Infineon) the Institute of High Energy Physics of the Austrian Academy of Sciences (HEPHY) developed planar silicon strip sensors in p-on-n technology. This work presents the first results from a beam test of strip sensors manufactured by Infineon.

© 2015 CERN for the benefit of the Authors. Published by Elsevier B.V. This is an open access article under the CC BY license (<http://creativecommons.org/licenses/by/4.0/>).

1. Introduction

The planned high luminosity upgrade of the LHC accelerator (HL-LHC) at the beginning of the next decade will significantly increase the number of particles traversing the experiments. By then, the existing tracking detectors will have reached the end of their lifetime due to irradiation damage. Therefore new systems have to be built, which will have to cope with the higher density of particle tracks and the increase in radiation. The new outer tracking detectors for the ATLAS and CMS experiments will both utilise the same basic sensor technology – silicon sensors produced in a standard planar production process (see eg. [1,2]).

The demand of silicon sensors needed for the construction of the trackers for the two mentioned LHC experiments alone might already exceed the production capabilities of companies and institutes which are available today. To facilitate the timely production of sufficient sensors, the Institute of High Energy Physics in Vienna (HEPHY) has engaged in a cooperation with Infineon Technologies Austria AG (Infineon) to develop a production process for silicon sensors. The development is in progress since late 2009 and in 2012 a first prototype batch of wafers has

been delivered to HEPHY. The sensors and test structures were electrically characterised at the institute and later tested in a particle beam at CERN's SPS accelerator. This paper presents the results from the beam tests of one species of strip sensors produced with the first batch.

2. Sensors and modules

A first prototype batch of silicon strip sensors as seen in Fig. 1 was designed at HEPHY and produced at Infineon's production site in Villach. It was intended to recreate the current state-of-the-art in silicon strip detectors as they are used for example in the outer tracker of the CMS experiment at the LHC accelerator [3]. An overview of the specifications for the bulk material and the strip sensors can be found in [4] together with the results from the electrical characterisation of the sensors.

The type of sensor investigated in this paper is the so-called SensorSTS, which is an AC-coupled strip sensor with outer dimensions of $50 \times 22.5 \text{ mm}^2$ produced in p-on-n technology. It is composed of 256 strips at a pitch of $80 \mu\text{m}$ and a width of $20 \mu\text{m}$.

The sensors were mounted on a carrier made from a plastic material. A PCB with two APV25 readout chips together with a small pitch adapter, a glass substrate with aluminium traces, is attached to the carrier as well. The readout chips and the sensor

* Corresponding author. Tel.: +43 1 5447328 36.

E-mail address: marko.dragicevic@oeaw.ac.at (M. Dragicevic).

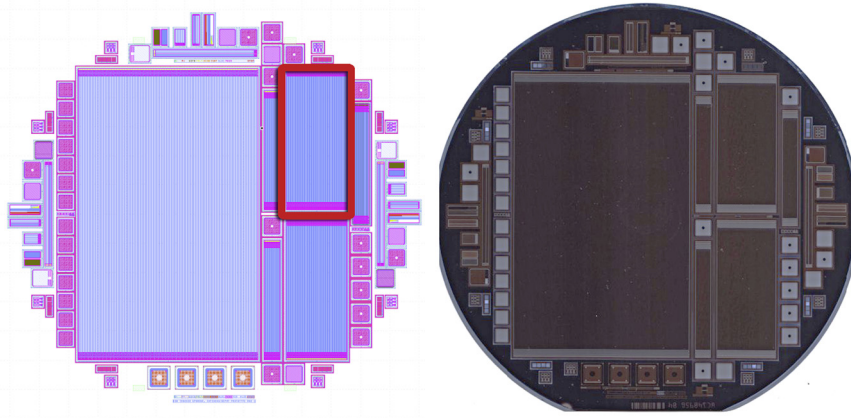


Fig. 1. Design of the full wafer layout (left) and the final wafer as produced by Infineon (right). The so-called SensorSTS used in the beam tests is marked in the left picture.

strips are electrically connected to the pitch adapter using wire bonds while a thin isolated wire connects the high voltage line on the PCB to the backside of the sensor. A flatband cable can be plugged into a connector at the edge of the PCB to send and receive signals from the backend readout system and provide the high voltage to operate the sensor. The assembly can be closed with a cover where both, carrier and cover, have an opening to expose the sensor. The full assembly, as seen in Fig. 2, is called a module.

3. Testbeam setup

The sensor was exposed to a 120 GeV/c hadron beam from the SPS accelerator at CERN. The beam was wide enough to illuminate the full width of the sensors. The sensor was operated at a bias voltage of 300 V which is well above full depletion ($V_{fd} \approx 250$ V) and the current was monitored during operation. The module was placed on an xy-table to select the illuminated area of the sensors where the beam was always perpendicular to the sensor plane. A single scintillator read out by a photomultiplier provided the trigger signal. The APV25 chips were read out by a prototype system for the Belle II SVD which is described in [5].

Two runs were performed, collecting approximately 340 k events in the first run and 150 k events in the second run. In the first run the upper part of the sensor (near the readout chips) was targeted, while in the second run the lower part (far from the readout chips) was targeted. The module was subsequently irradiated at SCK•CEN in Mol, Belgium with a dose of 700 kGy of gammas from a ^{60}Co source at a dose rate of 25 kGy/h. The module was then put back into the same beam at the SPS for a third run collecting about 300 k events where the sensor was approximately hit at the centre along the strips.

4. Results

4.1. Analysis software

A custom made analysis software has been implemented in the ROOT framework [6] to analyse the data. It calculates pedestals and noise means for each strip and for each run from the first 600 events which were taken with a random trigger. The common mode noise is calculated subsequently and subtracted from the noise for each strip. Strips showing excessive noise are excluded from the analysis. Clusters are built from seed strips that exceed five times the strip noise and neighbouring strips are added to the cluster as long as they are above 3 times the strip noise.

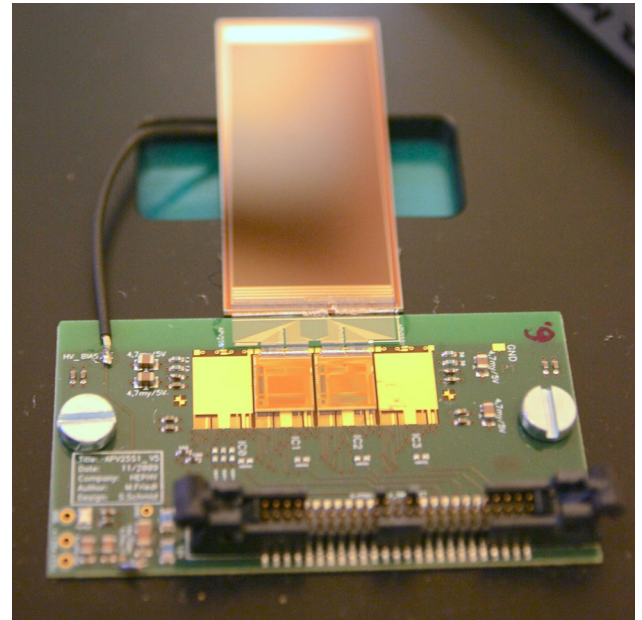


Fig. 2. Picture of a module. The cover has been removed to see the components inside the assembly: the sensor and the PCB containing the pitch adapter, two APV25 readout chips and a connector.

4.2. Expectations from electrical measurements

As reported in [4] the sensors of the first batch produced by Infineon suffer from a zone of weak strips. For the SensorSTS (80 μm pitch) used in this beam test, this zone is larger than for the SensorSTL (120 μm pitch) reported in the mentioned paper and spans from strip 222 to 238. The poor results in the electrical measurements could originate from bad strip isolation. This in turn might be caused by low mobility charge carriers introduced during the production or at a later stage. These charges could form an accumulation layer between the strips at the interface between the bulk silicon and the silicon dioxide, effectively lowering the resistance between strips. If this is the case, certain results from the beam test must show differences for strips inside and outside the affected weak area.

Irradiation with gammas should introduce additional fixed charge carriers inside the oxide between strips. They would influence the potential charge carriers located at Si–SiO₂ interface to the point where they could even neutralise the previously existing charge and mitigate the detrimental effect on the strip isolation.

4.3. Beam profile

A flat profile over all strips has been achieved for the first two runs as seen in Fig. 3. A few bad strips are seen at the left edge of the module and at around strip numbers 25 and 50. In run 3 (after irradiation) the sensor was only exposed to the edge of the beam except for the leftmost region which was already out of the trigger window set by the scintillator due to some misalignment as seen

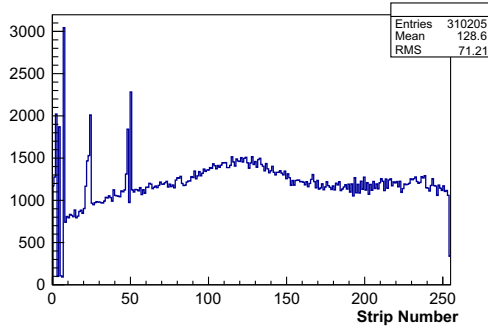


Fig. 3. Beamprofile for run 1.

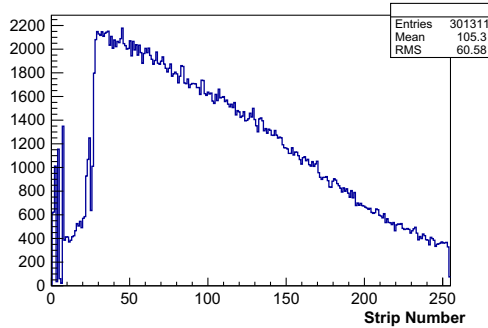


Fig. 4. Beamprofile for run 3 after irradiation.

in Fig. 4. Nevertheless, this should not influence the results as the weak and good regions are sufficiently well exposed to the beam.

4.4. Cluster widths

Electron-hole pairs are created along the track of a charged particle in a silicon strip sensor. The distribution of charge carriers inside the bulk depends on the inclination of the track to the sensor plane, which in the investigations described here was always perpendicular. The created charge carriers are then drifting towards the strips and the sensor backside according to the electrical field within the bulk. The clouds of electrons and holes are spread by diffusion and are collected by one or several strips (holes for a p-on-n sensor or electrons for an n-on-p sensor). The APV25 used in the module for these investigations is an analogue readout chip and can therefore measure the amount of charge which is collected by each strip. The sharing of charges created by a single incident particle depends mainly on the sensor thickness and the geometry of the strips (pitch and width). Furthermore, the signal is also shared between strips due to capacitive coupling.

The combined effects of charge sharing and capacitive coupling are seen in the results of a beam test for instance in the number of strips which are associated to a cluster. In essence, the cluster width gives the number of strips within a cluster which originated from the charge created by a single incident particle. For the geometry of a SensorSTS we would assume an average cluster width close to one. A more in-depth analysis on hit reconstruction in silicon strip sensors can be found in [7].

Following the assumption that the strip isolation in the weak region of the sensor is degraded, this would in turn cause unwanted resistive sharing of charge between strips and therefore increase the cluster width. In Figs. 5 and 6 this is clearly seen in both runs where clusters tend to be significantly wider in the weak area.

After irradiation with gammas, the cluster width distribution is identical over the full sensor as seen in Fig. 7. This result gives further support to the hypotheses formulated in Section 4.2.

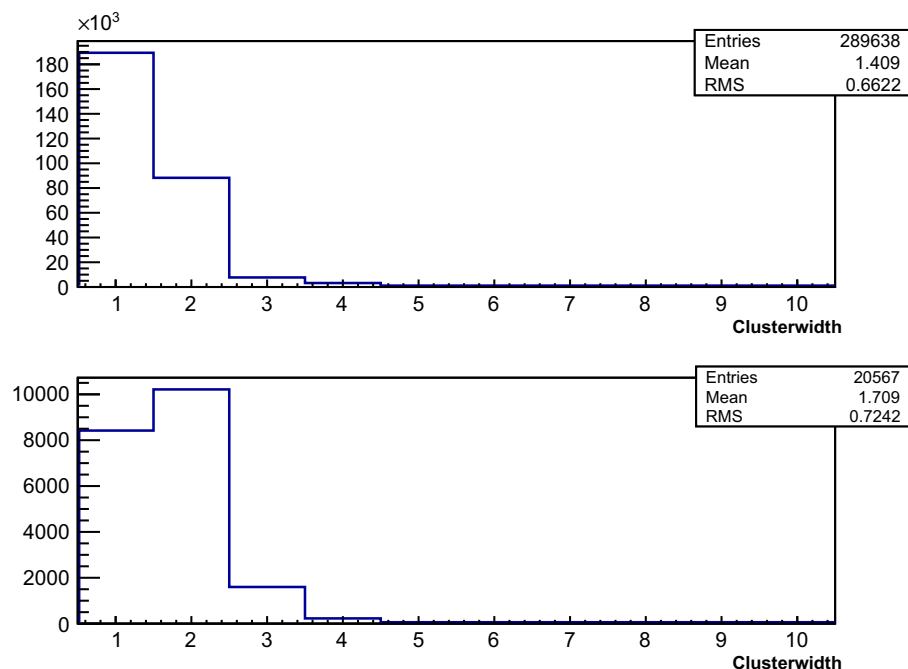


Fig. 5. Cluster width measured for strips in the good areas (upper) and inside the weak area (lower) in run 1. The expected average cluster width would be close to one.

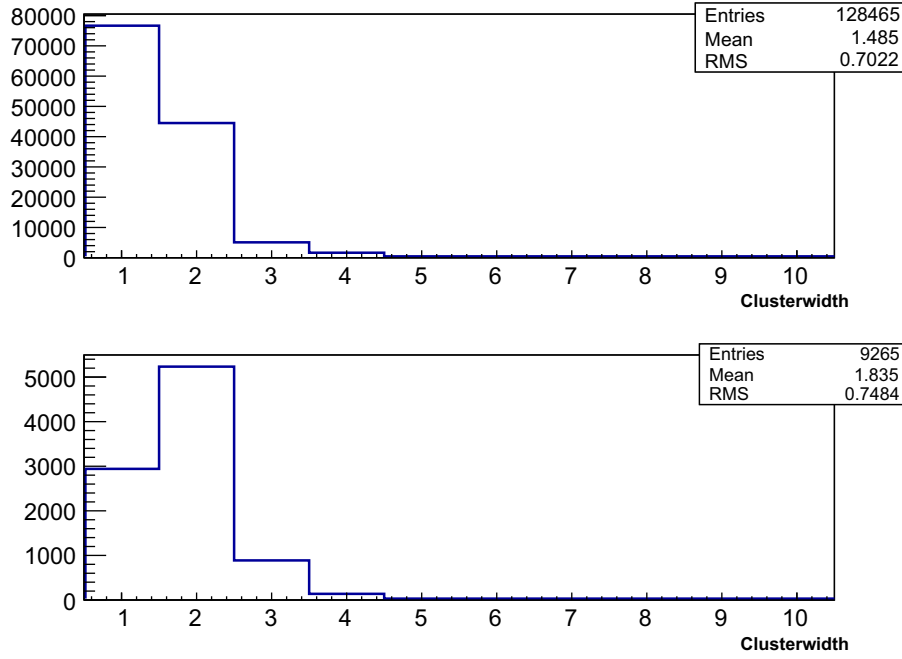


Fig. 6. Cluster width measured for strips in the good areas (upper) and inside the weak area (lower) in run 2. The expected average cluster width would be close to one.

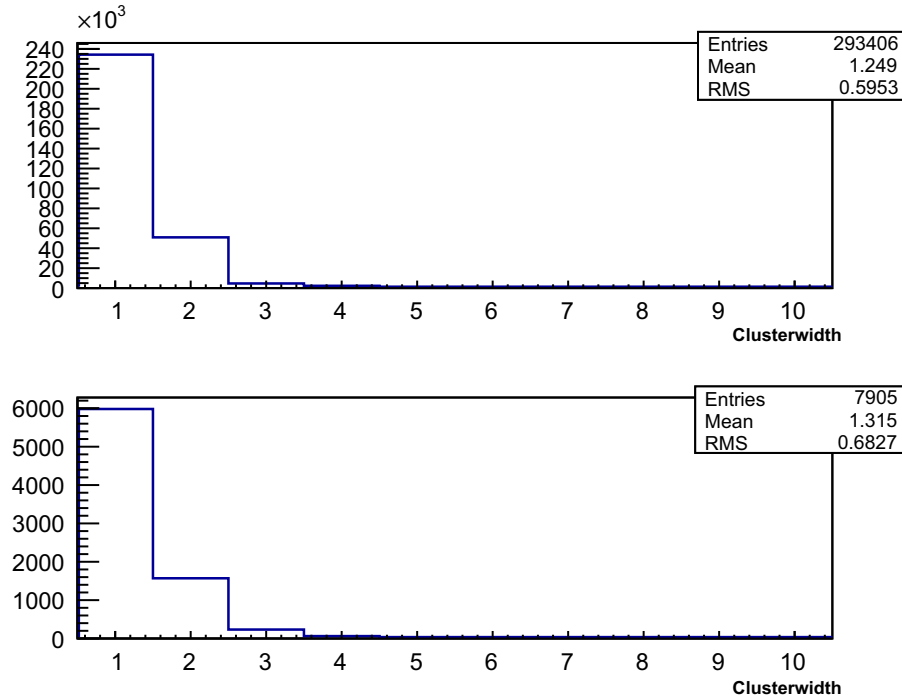


Fig. 7. Cluster width measured for strips in the good areas (upper) and inside the weak area (lower) in run 3 after gamma irradiation.

4.5. η distribution

The η distribution shows the distribution of the collected charge between neighboring strips according to

$$\eta = \frac{S_L}{S_L + S_R} \quad (1)$$

where $S_{L,R}$ are the highest strip signal of a cluster and its higher neighbour. The tails to the left and right of 0, 1 are from charge that is lost to the neighboring strips but does not fulfill the requirements to be included in the cluster (single strip hits).

The tracks of the incident particles are certainly uniformly distributed between the strips, but due to small size of the diffusion cloud of the holes (in the order of 10 μm), the nonuniform configuration of the electric field towards the strips and capacitive coupling of neighbouring strips, the distribution is distorted. This means that only the charge created by particles which traverse the sensor near the centre between strips is equally distributed between strips. Otherwise the charge mainly tends to get collected by the nearer strip. The η distribution can be used to correct for this effect and reconstruct the true position of the incident particle with much higher accuracy. More information can again be found in [7].

Assuming bad strip isolation for our strips within the weak region, the η distribution should be distorted further. The additional resistive coupling would lead to a sharing of charges between neighbouring strips. As seen in Fig. 8 two additional peaks appear near the strip edges compared to the expected distribution for strips in the good areas. In Fig. 9 the distribution shows a large peak in the centre between the strips, which resembles the situation of a sensor

with an additional intermediate strip which is not read out. Both results further support the assumption that charge is shared due to a low resistive path between strips.

The difference seen in the η distribution between run 1 and 2 can only originate from the beam hitting different parts of the sensor. The resistive charge sharing effect seems to be more pronounced when the strips are hit far from the readout chips as

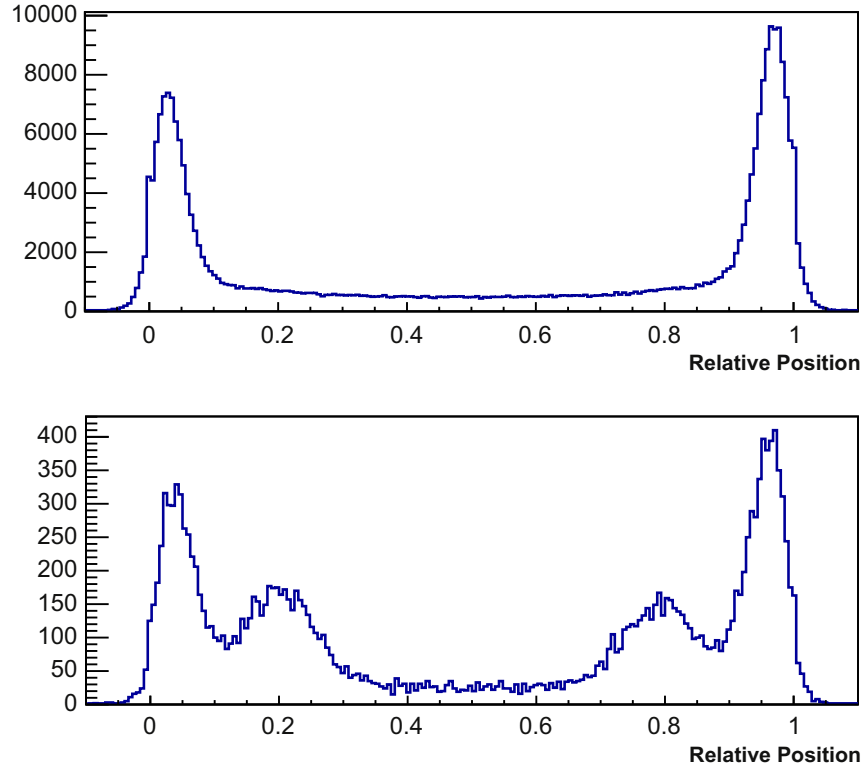


Fig. 8. η distribution measured for strips in the good areas (upper) and inside the weak area (lower) in run 1.

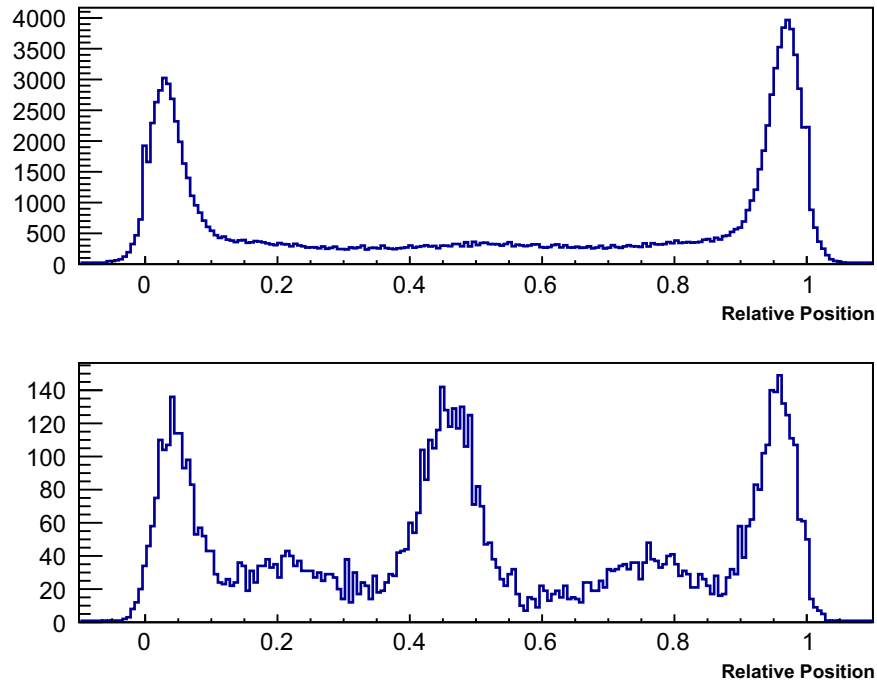


Fig. 9. η distribution measured for strips in the good areas (upper) and inside the weak area (lower) in run 2.

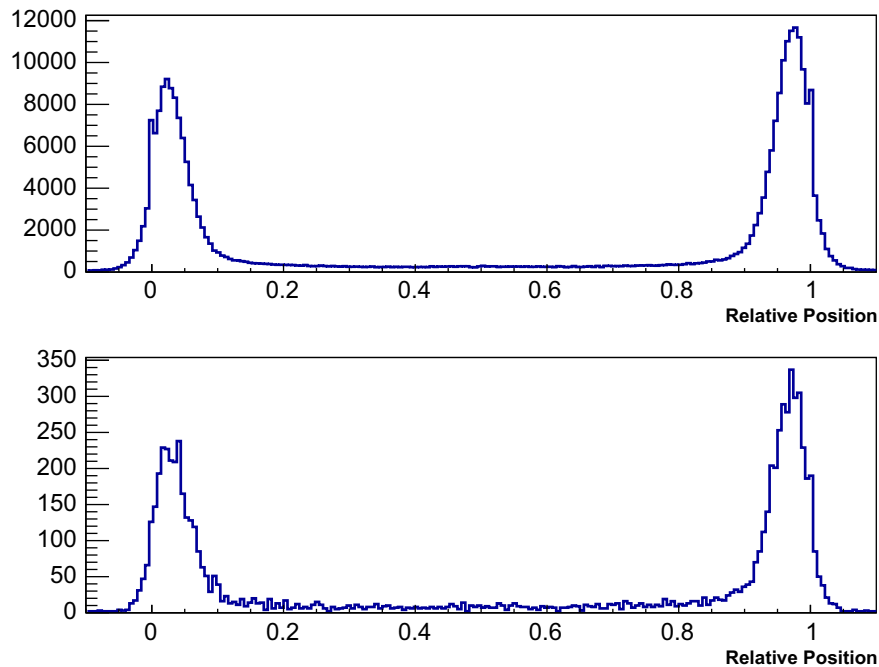


Fig. 10. η distribution measured for strips in the good areas (upper) and inside the weak area (lower) in run 3 after gamma irradiation.

in run 2. Looking back more closely to the cluster widths in Figs. 5 and 6, a similar effect is seen, where again the shift towards larger clusters is more pronounced in run 2. This suggests that the resistive charge sharing effect is also localised at a small region along the strip and not spread over the full length (Fig. 10).

5. Summary and conclusion

The first batch of strip sensors produced by Infineon showed an overall promising quality. Nevertheless the electrical characterisation revealed a small area of weak strips, which was seen on all sensors. We assume that bad strip isolation in the weak area is the actual reason for the results seen in the measurements. This could be caused by low mobility charge carriers introduced during manufacturing.

The cluster width and η distributions for strips within and outside of the weak area confirm this assumption. Furthermore, particles traversing the sensor at different locations along the strip cause differences in this distribution which can be explained by a nonuniform strip isolation.

After irradiation with gammas, the strips in the weak area show the same behaviour as strips in good areas of the sensor.

This could be explained by a compensation effect due to the oxide charges created by the gamma irradiation further supporting our assumptions.

Additional investigations are planned to determine if the low mobility charge carriers can be manipulated or removed by heat treatment, by exposition to water or by irradiation with hadrons.

References

- [1] D. Abbaneo, *Journal of Instrumentation* 6 (2011) C12065.
- [2] K. Hara, Y. Ikegami, *Nuclear Instruments and Methods in Physics Research Section A* 731 (2013) 242.
- [3] J.-L. Agram, et al., *Nuclear Instruments and Methods in Physics Research Section A* 517 (1–3) (2004) 77.
- [4] M. Dragicevic, et al., *Qualification of a new supplier for silicon particle detectors*, *Nuclear Instruments and Methods in Physics Research Section A*, *Nuclear Instruments and Methods in Physics Research Section A* 732 (2013) 74.
- [5] M. Friedl, C. Irmeler, M. Pernicka, Readout and data processing electronics for the Belle-II silicon vertex detector, in: *Proceedings of the TWEPP 2009*, vol. 6, 2009, pp. 417–421.
- [6] R. Brun, F. Rademakers, *Nuclear Instruments and Methods in Physics Research Section A* 389 (1–2) (1997) 81 (see also <http://root.cern.ch>).
- [7] R. Turchetta, *Nuclear Instruments and Methods in Physics Research Section A* 335 (1–2) (1993) 44.